

POLARIZED PROTONS AT RHIC

■ G. Bunce, J. Collins, S. Heppelmann, R. Jaffe, S.Y. Lee, Y. Makdisi, R.W. Robinett, J. Soffer, M. Tannenbaum, D. Underwood and A. Yokosawa

■ Abstract

Recent technical developments in the acceleration of polarized protons, using so-called Siberian snakes, now allow for the achievement of polarized proton–proton collisions at collider energies. We review the machine physics of achieving such collisions and describe a comprehensive program of spin physics which can be carried out at the RHIC facility using polarized pp collisions.

1. Introduction

The hugely successful program of QCD and electroweak tests at the hadron colliders at CERN and FNAL has provided a wealth of information on the Standard Model of particle physics. Tests involving jets (single and multi-jet events), direct photons, Drell–Yan weak boson production, and heavy quark and quarkonium production have probed the structure of the QCD hard-scatterings, often beyond leading order, and have yielded additional information on the parton structure of the proton itself.

One aspect of our understanding which has not benefitted from such experiments at high-energy colliders, however, is the area of spin physics, both the spin structure of the proton itself and the spin-dependence of the fundamental interactions.

Polarized pp collisions, which can address both issues, have previously been restricted to relatively low-energy (by collider standards) fixed-target experiments. So, spin, although historically central to the development of particle physics, has occasionally been relegated to a “soft physics” compartment in our field, despite indisputably large effects seen in many different experiments. At issue has been the interpretation whether a perturbative QCD analysis is possible or whether a complete understanding of non-perturbative effects is necessary.

With the successful tests of the Siberian snake concept [1], it now seems clear that a polarization option at a hadron collider, especially the Relativistic Heavy Ion Collider (RHIC) at BNL, is now a definite possibility [2–5]. A comprehensive program of experiments at such a facility would allow one to measure the spin-dependent parton distributions of the proton (both longitudinal and transverse) and would help to resolve any “spin crisis” raised by some theoretical interpretations of the much discussed Electromagnetic Calorimeter (EMC) experiments on polarized lepton–nucleus scattering [6]. Furthermore, it would provide fundamental spin tests of QCD and the electroweak interactions not accessible to unpolarized colliders, probing the helicity structure of the matrix elements of the fundamental hard scattering processes. Finally, the high energy and luminosity of such a machine would guarantee that a perturbative QCD approach would be applicable and would also be sufficient to

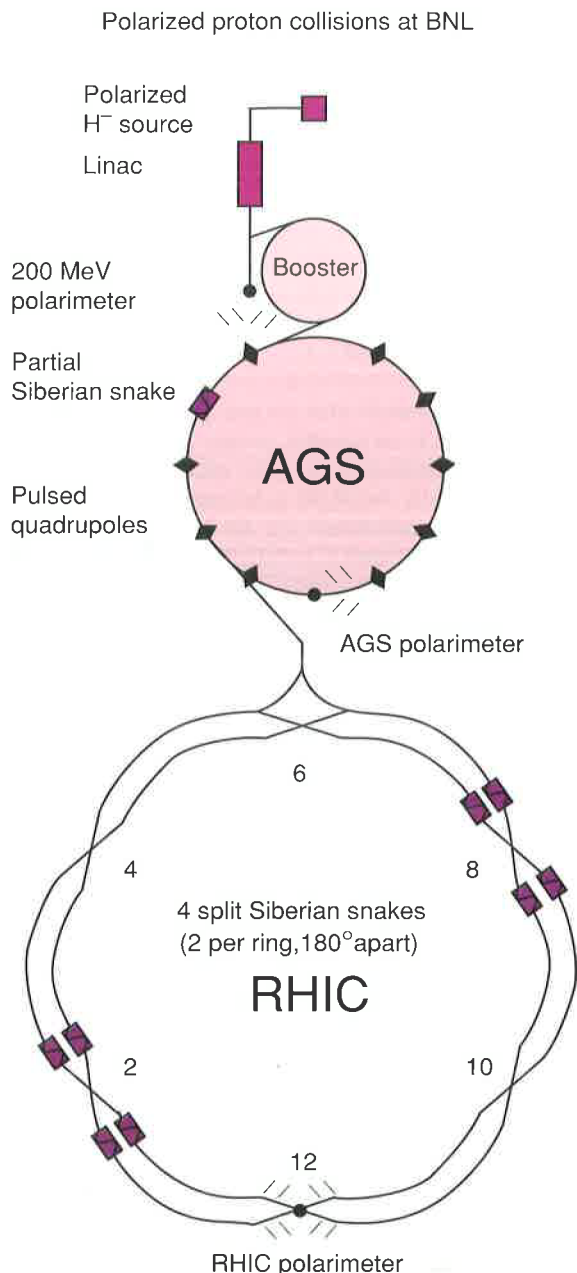
produce high p_T jets and weak bosons copiously while at the same time ensuring that the contributing quark processes are in a region of documented high polarization. In these regards, a RHIC spin program will be unique.

Tests using polarized beams and targets at fixed-target energies involving direct photons and quarkonium production have been put forth as possible probes of the longitudinally polarized gluon distributions. The relatively low energies involved at presently envisaged polarized fixed-target facilities put the proposed experiments near the limit of applicability of perturbative QCD. In contrast, polarized pp collisions at RHIC, at collider energies ($\sqrt{s} = 50 - 500$ GeV) and with high luminosity (reaching $\mathcal{L} = 2.10^{32}$ cm⁻²s⁻¹) would provide a huge sample of large transverse momentum events to which perturbative QCD would be just as applicable as at existing unpolarized machines. Furthermore, this can likely be achieved while providing $\sim 70\%$ polarization in each beam. Even with limited running time (say one month a year), this could yield well over 50 pb⁻¹ of data and so would allow for high statistics studies of QCD and electroweak phenomena [5] and their spin dependence at a previously unattained level.

Besides being of unquestioned importance in its own right, such a program of collider spin physics is a crucial step in the assessment of the possible importance of polarization options at future supercolliders such as SSC or LHC. Given the extent to which the particle-physics community is committed to high-energy collider physics, it is of utmost importance that the parton content of the proton, including its spin dependence, be understood and it seems that a polarized RHIC facility would be the ideal machine for economically pursuing this program.

Motivated by these possibilities, a number of experimentalists, particle and nuclear theorists, and machine physicists have formed the RHIC Spin Collaboration (RSC) [7] to develop a comprehensive and compelling program of spin physics for RHIC. Some aspects of the physics prospects for such a facility have been discussed elsewhere [4,8,9] and in this article we will review various components of the proposal to achieve a program of polarized pp collisions at the RHIC. In sect. 2 we describe

some of the technical considerations relevant for producing, storing and monitoring polarized proton beams of the proposed spin RHIC complex (fig. 1), while in sect. 3 we discuss in some detail the physics questions which can be addressed at such a



2

FIGURE 1

Proposed spin RHIC complex.

facility. We describe a program to map out the helicity-dependent parton distributions and to test the spin structure of the basic QCD interactions, as well as that of the electroweak theory using the unique tools provided by the existence of polarization information; we will also emphasize the importance of transverse spin asymmetries. In sect. 4, we discuss briefly some of the implications that the desired physics program may have for possible detectors and we give some concluding remarks.

2. Technical considerations of high-energy polarized beams

2.1 Polarized beam luminosity in RHIC with Siberian snakes

To achieve high-energy polarized proton collisions in RHIC, the AGS polarized proton source may be used. The source [10] produces $30 \sim 40 \mu\text{A}$ of H^- with 75–80% polarization in 500 μs pulses at a repetition rate of 5 Hz. The polarized H^- ions are accelerated to 200 MeV with an RFQ and 200 MHz with the Linac. Twenty pulses of H^- ions are strip-injected and accumulated in the AGS booster. Each bunch in the booster will contain $N_B = (1-3) \times 10^{11}$ polarized protons with normalized emittance about $\epsilon_N = 10 \pi$ mm-mrad depending on the harmonic number of the r.f. system used in the booster.

The accumulated proton bunch will be transferred and accelerated to 24 GeV in the AGS. During the acceleration, the polarization may be lost when the spin precession frequency $G\gamma$ (G is the Pauli anomalous g factor) is equal to the spin depolarizing resonance. These resonances occur at an integer (imperfection resonance) due to vertical closed orbit errors or at $kP \pm \nu_y$ (intrinsic resonance) due to the vertical betatron motion. Here, $P = 12$ is the superperiod of the AGS, $\nu_y = 8.8$ is the vertical betatron tune, and k is an integer. Traditionally, these spin depolarizing resonances are corrected by the tedious harmonic correction method for the imperfection resonances and the tune-jump method for the intrinsic resonances.

In an approved experiment [11] at the AGS to be performed in 1993, the feasibility of polarized proton acceleration by using a 5% solenoid Siberian snake will be tested. Previous experiences with polarized proton acceleration in the AGS indicate that a 5% snake is indeed sufficient to overcome imperfection resonances without using the harmonic correction method. The remaining six important intrinsic resonances can be corrected by the tune-jump method. At 24 GeV kinetic energy, the polarized protons are transferred to the RHIC. The transfer line between the AGS and the RHIC is spin-transparent at this energy.

In the RHIC, spin depolarizing resonances can be overcome with two Siberian snakes [1] located symmetrically in each of the RHIC rings. Using the split snake configuration [12] (fig. 2), proton collisions with longitudinal or transverse polarization can be achieved without using additional spin rotators. The maximum spin depolarizing resonance strength is found to be ~ 0.4 for a normalized emittance of 10π mm-mrad.

process $pA \rightarrow pA\pi^0$ can be related via the Primakoff effect to low-energy photoproduction, i.e. $\gamma p \rightarrow \pi^0 p$. The amplitude ψ for diffractive production from a nucleus with charge Z and atomic number A can be written as [15]

$$\int |\Psi|^2 d\phi = \frac{z^2 \alpha}{p_{\perp}^2} \left(\frac{2M_A}{s_{\pi p} - m_p^2} \right)^2 \left(A \frac{d\sigma}{d\Omega} \right)_{\gamma p \rightarrow \pi^0 p}, \quad (1)$$

where A is the photoproduction asymmetry at the given value of p_{\perp} and $s_{\pi p}$. Results of measurements in $\gamma p^{\uparrow} \rightarrow \pi^0 p$ at the γp kinetic energy of 600 MeV show that the photoproduction asymmetry is $\sim 90\%$ at $\theta_{c.m.} \approx 90^\circ$ and $m_{p\pi^0} = 1.4 \text{ GeV}/c^2$.

The asymmetry of the nuclear coherent Coulomb π^0 production process was measured [17] for the first time with the use of the 185 GeV/c FNAL polarized-proton beam. The apparatus consisted of a lead-glass calorimeter for π^0 detection and a magnetic spectrometer for the scattered protons. A large asymmetry in the region of $|t'| < 0.001 \text{ (GeV}/c)^2$ and $1.36 < M(\pi^0 p) < 1.52 \text{ GeV}/c^2$ was observed for the reaction $p + \text{Pb} \rightarrow p + \pi^0 + \text{Pb}$, where the Coulomb process is predominant. Here $t' = t - (M^2 - m^2)^2/4 P_L^2$, where t is the square of the momentum transfer carried by the virtual photon, m is the proton mass, and P_L the momentum of the incident proton. The expected null asymmetry was observed in the larger $|t'|$ region where the diffractive-dissociation process is predominant.

The observed ϕ angle dependence of the coherent π^0 production process may be expressed as $1 + (fT(\theta)P_B) \cos\phi$, where the parameter f is a dilution factor caused by the diffractive dissociation. The raw asymmetry at ϕ is obtained as

$$A(\phi) = \frac{N^{\uparrow}(\phi) - N^{\downarrow}(\phi)}{N^{\uparrow}(\phi) + N^{\downarrow}(\phi)} = fT(\theta)P_B \cos\phi, \quad (2)$$

where $N^{\uparrow}(\phi)$ and $N^{\downarrow}(\phi)$ are the number of events at ϕ for the up and down spin direction of the incident proton, respectively. The asymmetry parameter ε is obtained by fitting the observed values of $A(\phi)$ as shown in fig. 3 with the functional form $A(\phi) = \varepsilon \cos\phi$.

The measured asymmetry for the Coulomb process is consistent with the analyzing power of the π^0 production process deduced from existing low-energy $\gamma + p \rightarrow \pi^0 + p$ data. The results demonstrate that the Primakoff process is useful for the measurement of proton and antiproton polarization at high energy.

- Coulomb-nuclear interference (CNI) polarimeter

Several authors since Schwinger [18] have indicated non-zero polarization in the Coulomb-nuclear interference region in nucleon-nucleon scattering. This polarimeter is to measure the interference term of the non-flip amplitude and the electromagnetic spin-flip amplitude. The proton polarization arising from the interference is $P \approx 5\%$ at $|t| = 2 \cdot 10^{-3} \text{ (GeV}/c)^2$ and is energy independent [19].

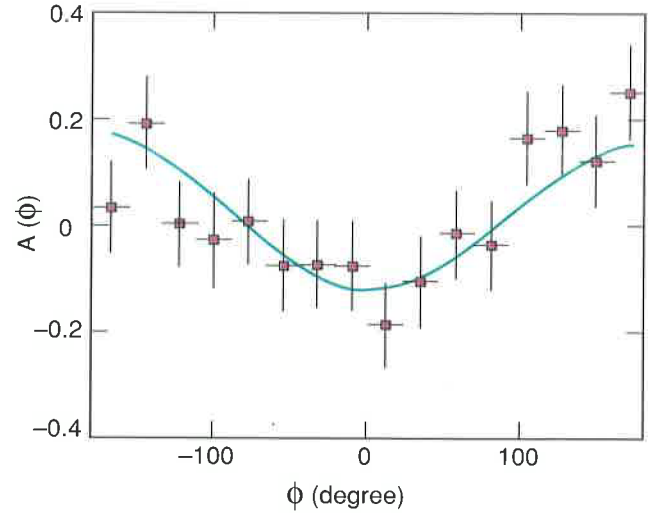


FIGURE 3

The observed values of $A(\phi)$ from ref. [17].

The analyzing power A_N of pp, proton-hydrocarbon and antiproton-hydrocarbon scattering in the Coulomb-nuclear region was earlier measured with use of the 185 GeV/c FNAL polarized-proton and polarized-antiproton beams [20]. For the elastic scattering at small $|t|$, a set of scintillation counters was utilized to detect the recoil proton which stops within a very short range in the scintillator. The results at $|t| \sim 0.003 \text{ (GeV}/c)^2$ show the value $A_N = (2.4 \pm 0.9)\%$ with the polarized-proton beam, and $A_N = (-4.6 \pm 1.9)\%$ with the polarized-antiproton beam (both on a hydrocarbon target), and also $A_N = (4.5 \pm 2.8)\%$ of pp scattering. These results are consistent with predictions [21–23] based on Coulomb-nuclear interference.

Recently a new CNI target consisting of trans-stilbene crystals (diphenylethylene, $C_{14}H_{12}$) was used [24]. This made possible to reduce large background at small $|t|$ region by using this material that possesses pulse-shape discrimination characteristics. Preliminary results on the pp analyzing power are shown in fig. 4 together with the calculated values.

- Sizeable asymmetries in π^0 , π^+ and π^- inclusive production at large x_F

Asymmetry measurements (A_N) on the x_F dependence at 200 GeV/c covering p_{\perp} up to 2 GeV/c were carried out [25]. A_N values in the $p^{\uparrow}p$ reaction are consistent with zero up to $x_F = 0.3$ or so, and then linearly increase up to the absolute value of 40% near $x_F = 1.0$ as shown in fig. 5. These effects can be applied to the design of beam polarimeters and beam-polarization monitors.

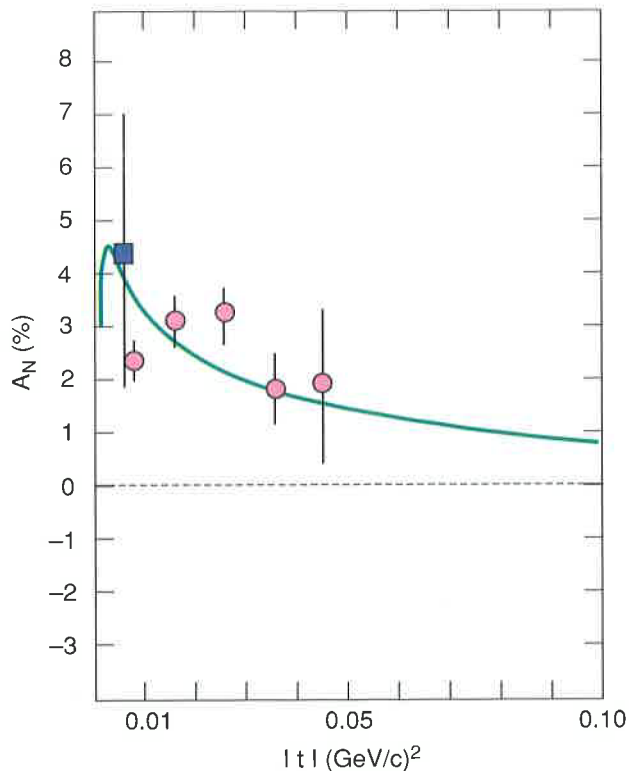


FIGURE 4

Analyzing power in the Coulomb-nuclear interference region.

3. Physics issues for a polarized collider

3.1 Measuring parton helicity distributions in a polarized proton(*)

Fundamental interactions at short distances which are probed in pp collisions at high energies, involve hard scattering of quarks and gluons. Let us consider the general hadronic reaction

$$a + b \rightarrow c + X, \quad (3)$$

where c , in the cases we will study below, is either a well-defined particle (hadron or gauge boson) or a single jet. In the hard scattering kinematic region, the cross section describing reaction (3) reads, in the QCD parton model, provided factorization holds as

$$d\sigma(a + b \rightarrow c + X) = \sum_{ij} \frac{1}{1 + \delta_{ij}} \int dx_a dx_b \left[f_i^{(a)}(x_a, Q^2) f_j^{(b)}(x_b, Q^2) d\hat{\sigma}_{ij} + (i \leftrightarrow j) \right]. \quad (4)$$

(*) This discussion follows from ref. [8].

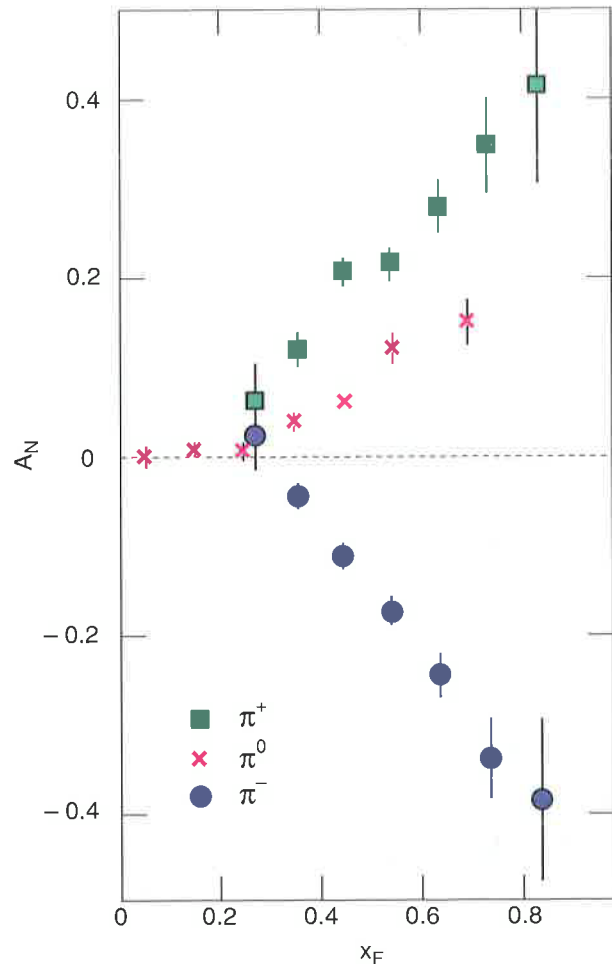


FIGURE 5

A_N versus x_F for π^+ , π^- and π^0 data from ref. [25].

The summation runs over all contributing parton configurations, the $f(x, Q^2)$ are the parton distributions, directly extracted from deep inelastic scattering for quarks and antiquarks, and $d\hat{\sigma}_{ij}$ is the cross section for the interaction of two partons i and j which can be calculated perturbatively, some of which are given in ref. [26]. If we consider the reaction (3) with *both* initial hadrons longitudinally polarized, one useful observable is the *double* helicity hadron asymmetry A_{LL} defined as

$$A_{LL} = \frac{d\sigma_{a(+)b(+)} - d\sigma_{a(+)b(-)} - d\sigma_{a(-)b(+)} + d\sigma_{a(-)b(-)}}{d\sigma_{a(+)b(+)} + d\sigma_{a(+)b(-)} + d\sigma_{a(-)b(+)} + d\sigma_{a(-)b(-)}}, \quad (5)$$

which reduces to

$$A_{LL} = \frac{d\sigma_{a(+)\bar{b}(+)} - d\sigma_{a(+)\bar{b}(-)}}{d\sigma_{a(+)\bar{b}(+)} + d\sigma_{a(+)\bar{b}(-)}}, \quad (5')$$

if parity is conserved because $d\sigma_{a(\lambda)\bar{b}(\lambda')} = d\sigma_{a(-\lambda)\bar{b}(-\lambda')}$. It is given by

$$A_{LL} d\sigma = \sum_{ij} \frac{1}{1 + \delta_{ij}} \times \left[dx_a dx_b \left[\Delta f_i^{(a)}(x_a, Q^2) \Delta f_j^{(b)}(x_b, Q^2) \hat{a}_{LL}^{ij} d\hat{\sigma}_{ij} + (i \leftrightarrow j) \right], \quad (6)$$

assuming the factorization property, where $d\sigma$ is given by eq. (4) and \hat{a}_{LL}^{ij} denotes the corresponding subprocess asymmetry for initial partons i and j . The $\Delta f(x, Q^2)$ are the parton helicity asymmetry defined as

$$\Delta f(x, Q^2) = f_+(x, Q^2) - f_-(x, Q^2), \quad (7)$$

where f_{\pm} are the parton distributions in a polarized hadron with helicity either parallel (+) or antiparallel (-) to the parent hadron helicity. Recall that the unpolarized parton distributions are $f = f_+ + f_-$. If only *one* initial hadron is polarized, say "a", another interesting observable is the *single* helicity asymmetry defined as

$$A_L d\sigma = \frac{d\sigma_{a(-)\bar{b}(-)} - d\sigma_{a(+)\bar{b}(+)}}{2}, \quad (8)$$

a quantity for which one can write an expression similar to eq. (6), provided $\Delta f_j^{(b)} \rightarrow f_j^{(b)}$ and $\hat{a}_{LL}^{ij} \rightarrow \hat{a}_L^{ij}$, the single helicity subprocess asymmetry. A_L is expected to vanish unless some subprocesses involve parity-violating interactions i.e. $\hat{a}_L^{ij} \neq 0$. If *both* initial beams are polarized, it is also possible to define another parity violating asymmetry namely

$$A_{LL}^{PV} d\sigma = \frac{d\sigma_{a(-)\bar{b}(-)} - d\sigma_{a(+)\bar{b}(+)}}{2}, \quad (8')$$

which can be for special cases about twice as big as A_L . We will then remember that, if at the RHIC one achieves the same luminosity with polarized and unpolarized proton beams, it will be certainly more advantageous to measure A_{LL}^{PV} rather than A_L .

Both for polarized and unpolarized parton distributions, we will take a set in terms of a simple parametrization of their x and Q^2 dependences already used in ref. [26]. Concerning the gluon helicity asymmetry $\Delta G(x, Q^2)$ there is a standard choice (e.g. eq. (3.12) in ref. [26]) such that $\Delta G(x)/G(x)$ is only a few percent up to $x = 0.1$. Since the relevant kinematic region stands at small x values, it results that at small Q^2 , the integral $\Delta G = \int_0^1 \Delta G(x) dx$ is only 0.2 – 0.3 and it increases slowly with Q^2 . This choice means that one expects gluons to carry $\sim 25\%$ of the proton spin and until very recently there were no experimental facts to contradict this reasonable assumption. However, after the striking EMC result [27], in particular on the small x behaviour of the spin-dependent structure function $g_1(x, Q^2)$, several interpretations and

new pictures for the proton spin have been proposed, some of them, suggesting that the proton spin receives a large contribution from either the gluons ($\Delta G(x)$ large) or the sea ($\Delta \bar{q}(x)$ large). The presence of a large $\Delta G(x)$ or ($\Delta \bar{q}(x)$) might well imply a "no-lose theorem" for future polarized colliders, i.e. more polarization at small x than previously thought. Among these various possibilities, a suggestion, due to the existence of the anomaly of the axial-vector current, leads one to anticipate a $\Delta G(x)$ much larger than the standard choice, in particular in the small x region. Therefore, following ref. [28] we will also consider the simple parametrization

$$\Delta G(x, Q_0^2) = \begin{cases} G(x, Q_0^2) & x_c \leq x \leq 1 \\ (x/x_c) G(x, Q_0^2) & 0 \leq x \leq x_c \end{cases}, \quad (9)$$

which can lead to a much larger value of the integral ΔG than for the standard choice, the smaller x_c the larger ΔG . We will take $x_c \sim 0.2$ corresponding to $\Delta G \sim 2-3$, because this is the value which gives the best agreement with the $g_1(x, Q^2)$ data. Clearly, now gluons give a much too large contribution to the proton spin which ought to be balanced by a large orbital angular momentum. We have no very strong theoretical argument to prefer the standard form or this second choice (eq. (9)) and, of course, due to the lack of our knowledge other choices are equally possible. These two rather different forms of the gluon helicity asymmetry will allow us to study how much a given reaction is sensitive to ΔG , whose precise form can be only determined from future data at the RHIC.

Direct photon production at high p_T is a useful probe of the underlying parton-parton interactions and probably one of the cleanest reactions to study the perturbative regime, because the photon originates in the hard scattering subprocess and does not fragment. In the QCD parton model, in the absence of photon bremsstrahlung contributions, direct photons are produced via the $q\bar{q}$ annihilation subprocess $q\bar{q} \rightarrow \gamma g$ and the quark-gluon Compton subprocess $qg \rightarrow q\gamma$. The Compton subprocess has a positive \hat{a}_{LL} and leads to a contribution to A_{LL} , for $\vec{p} \vec{p}' \rightarrow \gamma X$, directly proportional to $\Delta G(x, Q^2)$. For the annihilation subprocess one has $\hat{a}_{LL} = -1$. First we note that given the high-designed luminosity at the RHIC, direct photon cross sections will be measurable up to fairly high p_T values. For the calculation of A_{LL} if one uses the standard distribution $\Delta G(x, Q^2)$ (eq. (3.12) of ref. [26]), one obtains a very small positive result, say at most (5–10)%. This reflects the dominance of the Compton subprocess and the small magnitude of A_{LL} is partly due to the fact that u quark-gluon and d quark-gluon lead to opposite sign effects. However, if instead one assumes a large distribution ΔG like in eq. (9) one gets the results displayed in fig. 6, where the error bar indicates the precision possible for a one month run at the nominal luminosity [5]. A_{LL} rises with p_T reaching values of the order of 20% or more for the production angle $\theta_{c.m.} = 90^\circ$ and much larger for $\theta_{c.m.} = 45^\circ$. So this shows that the p_T dependence

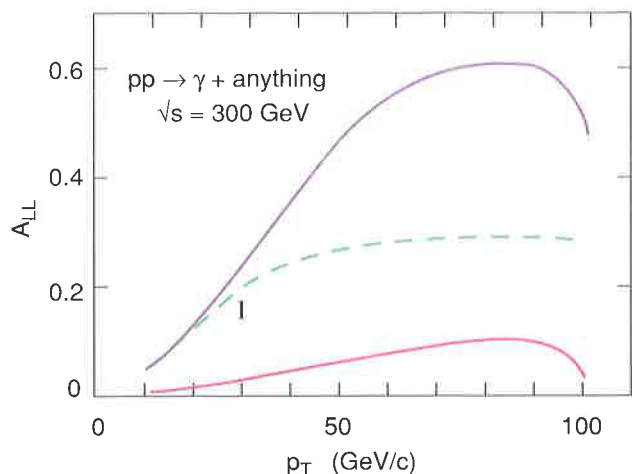


FIGURE 6

Predicted A_{LL} with a large ΔG for $\sqrt{s} = 300$ GeV as a function of p_T for two different values of the c.m. production angle: $\theta_{c.m.} = 90^\circ$ (dashed curve), $\theta_{c.m.} = 45^\circ$ (solid curve). The small-dashed curve corresponds to a standard ΔG and $\theta_{c.m.} = 90^\circ$. The error bar indicated the RHIC sensitivity at $p_T = 20$ GeV/c and for $\Delta y = 1$, $\Delta\phi = 2\pi$, $\Delta p_T = 1$ GeV/c bin [5].

of A_{LL} in direct production is very sensitive to the gluon polarization and that it should best be measured with photons of rapidity of the order of 1. In fig. 6 at very large p_T , A_{LL} is dropping off because in this kinematic region one feels the effect of the annihilation subprocess which gives a negative contribution to A_{LL} .

Unlike for direct photon production, in the case of single-jet production, many pure QCD subprocesses contribute and the event rate is substantially bigger. The main contributions are gluon-gluon scattering which largely dominate at low p_T , followed by gluon-quark scattering at medium p_T before reaching at very high p_T the dominance of quark-quark elastic scattering. For unpolarized cross sections, lowest-order QCD predictions are compatible with data obtained by UA1 and UA2 Experiment, given the large experimental uncertainties. One can hope to reduce the effect of these uncertainties (mainly systematic errors) by taking cross section ratios, so this is the reason why we believe it will be useful to study the behaviour of the asymmetry A_{LL} at the RHIC and possibly to detect the effect of a large gluon polarization. Since for all the dominant subprocesses the corresponding asymmetries \hat{a}_{LL}^{ij} are positive (except for quark-antiquark annihilation), we expect a positive A_{LL} . The results of the calculations for a jet produced at $y = 0$ are shown in fig. 7 at $\sqrt{s} = 600$ GeV versus p_T . If one uses the standard-gluon distribution $\Delta G(x, Q^2)$ one obtains a very small A_{LL} for $p_T < 50$ GeV/c which rises at higher p_T due to the effect of the quark polarization. However, if one uses a large gluon distribution $\Delta G(x, Q^2)$ (i.e. eq. (9)) for low p_T where gluons

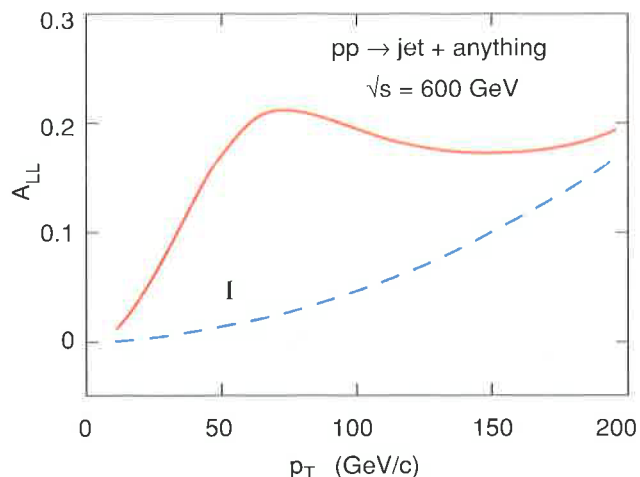


FIGURE 7

Predicted A_{LL} at $\sqrt{s} = 600$ GeV as a function of p_T , for a standard ΔG (dashed curve) and a large positive ΔG (solid curve). The error bar indicates the RHIC sensitivity at $p_T = 50$ GeV and for $\Delta y = 1$, $\Delta\phi = 2\pi$, $\Delta p_T = 1$ GeV bin [5].

dominate, A_{LL} reaches 20% or so. Therefore, the measurement of A_{LL} should allow us to discriminate easily between these two possibilities. One should emphasize that a detailed analysis of the behaviour of A_{LL} in various kinematic regions yields also useful constraints for a better determination of $\Delta u(x)$ and $\Delta d(x)$. Other processes which are known to be sensitive to the polarized gluon distribution include three-jet and two-jet plus photon production in polarized pp collisions [29].

Let us now consider the single W^\pm production with a large p_T , which is balanced by a hadronic jet. This is similar to the direct photon production we have studied above but in this case one should consider the quark-antiquark annihilation subprocesses $q_i\bar{q}_j \rightarrow Wg$ and the quark gluon Compton subprocess $q_i g \rightarrow q_j W$ with $i \neq j$. If the beams are polarized we recall that for the dominant Compton scattering $q_i(h) g(\lambda) \rightarrow q_j W$ the corresponding single asymmetry \hat{a}_L is 1 for polarized quarks and very close to 0 for polarized gluons. Therefore, the single hadron helicity asymmetry will be dominated by polarized quarks and not sensitive to ΔG . This is clearly shown in our results for A_L at $y = 0$ versus p_T displayed in fig. 8, where for W^+ one sees the trend of $\Delta u(x)/u(x)$ and for W^- the trend of $\Delta d(x)/d(x)$. At fixed p_T the effect decreases with increasing energy. Since the W are left-handed objects, the consideration of A_{LL}^{PV} would lead us to predict asymmetries about twice as big as these single helicity asymmetries and this is consistent with some earlier results.

3.2 Measuring quark transversity distributions in a polarized proton

A major reason for the renewed interest in deep inelastic spin physics is the recent progress in understanding and describing

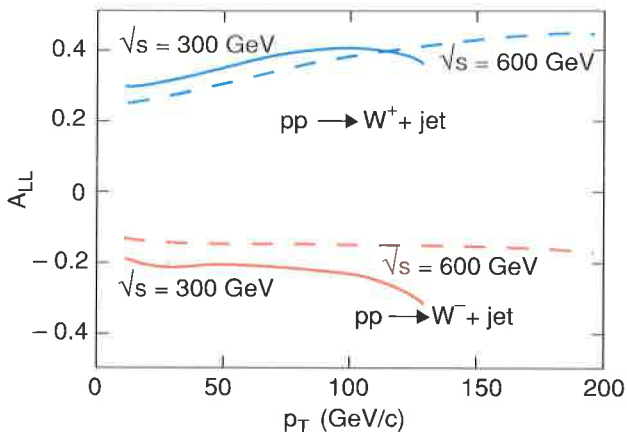


FIGURE 8

Predicted A_{LL} in $pp \rightarrow W^\pm + \text{jet}$ at $y = 0$ versus p_T for $\sqrt{s} = 300$ GeV (solid curves) and $\sqrt{s} = 600$ GeV (dashed curves).

transverse spin effects in inclusive hard processes [30]. The progress [31–36] affects both dominant, i.e. twist-2 and subdominant twist-3 contributions, unifies the description of spin in the parton model and suggests that nearly as much is waiting to be learned about nucleon structure from the study of transverse spin effects as from longitudinal.

To understand what is happening^(*) it is necessary to think about the role of *chirality* in perturbative QCD. If we ignore quark mass terms — a good approximation for u and d quarks, and an arguable one for s quarks — then the interaction of a quark with gluons, photons or W and Z bosons do not change the quark’s chirality, where chirality is the eigenvalue of the Dirac matrix γ_5

(*) This discussion follows ref. [36].

$$\gamma_5 q_L = -q_L, \quad \gamma_5 q_R = q_R, \quad (10)$$

for “left” and “right” handed quarks^(*). Even when the quarks are massless, chirality is not, however, a symmetry of QCD: it is broken by the vacuum state with the associated appearance of light pseudoscalar (Goldstone) bosons. This is a truly non-perturbative effect. Although we would not see it in perturbation theory, we will have to allow for it in our analysis of hard processes involving non-perturbative bound states like the nucleon.

With this in mind, let us look at the chiral structure of the parton description of deep inelastic scattering (fig. 9) and Drell–Yan production of lepton pairs (fig. 10). In both cases we show the diagram for the cross section. The *amplitude* is obtained by cutting it down the middle, as in fig. 9(a). The lepton lines which attach to photons are suppressed. In all diagrams it is clear that the chirality of the quark participating in the hard scattering process is conserved. In the case of deep inelastic scattering this has the *further* consequence that the *quark lines entering and leaving the nucleon are of a single chirality*. Only two independent quark–nucleon amplitudes enter the description of deep inelastic scattering^(**) — one involving left-handed quarks, the other right-handed — as shown in fig. 11. The average over chirality gives the quark momentum distribution $f_1(x, Q^2)$. The difference gives the chirality (or helicity) weighted quark momentum distribution $g_1(x, Q^2)$ measured at SLAC and by the EMC. $f_1(x, Q^2)$ can be measured with an unpolarized target. $g_1(x, Q^2)$ is the dominant (at large Q^2) contribution to the spin asymmetry from a longitudinally polarized target.

What happens when one measures the spin asymmetry from a transversely polarized target in deep inelastic scattering? A transversely polarized nucleon can be regarded as a superposition of longitudinally polarized states

(*) For massless quarks chirality and helicity coincide. For massive quarks, chirality remains exactly conserved at gauge boson vertices but helicity does not.

(**) For each flavour of quark or antiquark.

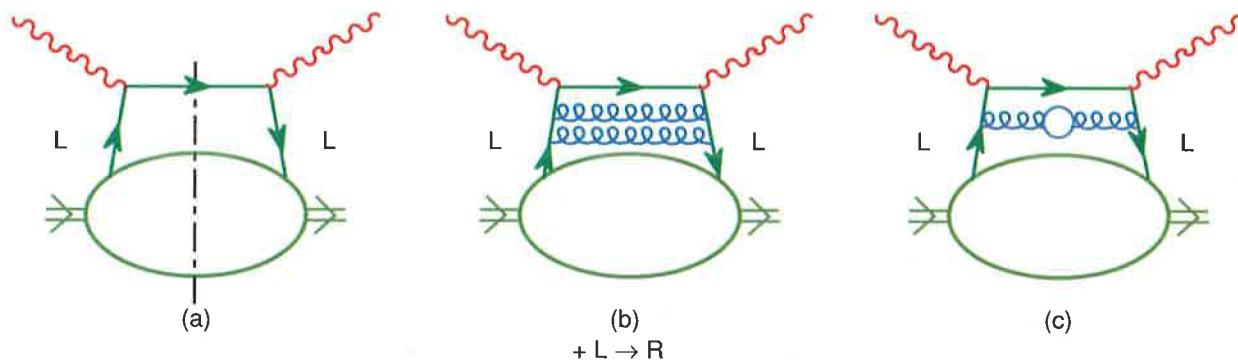


FIGURE 9

Chiral structure of deep inelastic scattering.

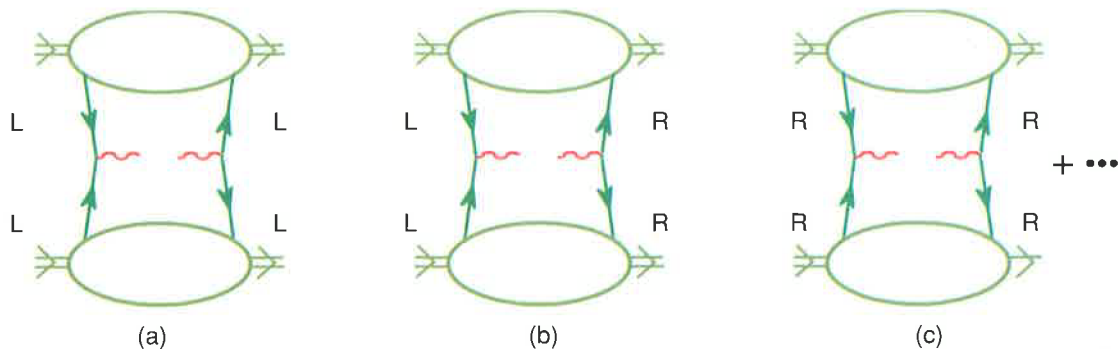


FIGURE 10

Chiral structure of Drell-Yan production of lepton pairs. No QCD radiative corrections are shown.

$$|\vec{p}_z, \pm \ell_x\rangle = \frac{1}{\sqrt{2}} (|\vec{p}_z, \ell_z\rangle \pm |\vec{p}_z, -\ell_z\rangle) . \tag{11}$$

For massless quarks, helicity and chirality coincide. But the transverse asymmetry measures an amplitude in which the nucleon helicity changes but in whose hard scattering the quark chirality does not change. This clash suppresses the process by a factor $1/\sqrt{2}$ [30]. The suppression arises because angular momentum conservation requires the quark-nucleon amplitudes in fig. 11 to vanish identically if the initial and final nucleon differ by helicity flip.

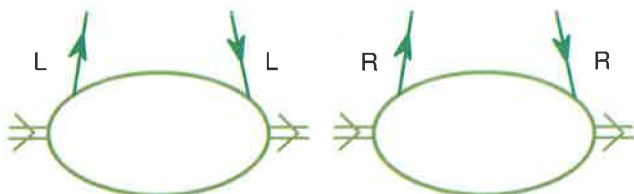


FIGURE 11

Left and right handed, chiral even quark distributions whose sum and difference give $f_1(x, Q^2)$ and $g_1(x, Q^2)$, respectively.

There are two main effects that cause the measured asymmetry not to vanish. First, effects proportional to m_q allow the quark helicity to flip without changing chirality, but such effects are suppressed by $m_q/\sqrt{Q^2}$. Second, hard gluon interactions allow the quark helicity to be transferred to gluons while preserving chirality. An example is shown in fig. 12. Analysis of these effects in QCD show that the extra-hard interaction always costs at least a factor of the order of $\Lambda_{\text{QCD}}/\sqrt{Q^2}$ [37]. The conclusion is that transverse spin effects in deep inelastic scattering, summarized by the structure function $g_2(x, Q^2)$, are suppressed by a factor of $\sim 1/\sqrt{Q^2}$. They are interesting probes of quark masses and quark-gluon interactions, but they are subdominant and not so easy to measure.

Now let us turn to Drell-Yan. As always, the quark chirality is conserved in the hard part of the diagram. However, it is clear from fig. 10(b) that the *chirality of the quark lines entering and leaving a given nucleon need not be the same*.

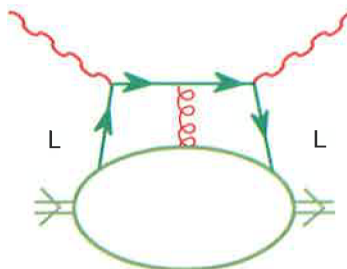


FIGURE 12

A hard gluon (twist-3) contribution to deep inelastic scattering. The quark's chirality is conserved but its helicity need not be.

This allows us to define a new quark distribution shown in fig. 13. One might, at first sight, think that chirality conservation at quark-gluon vertices in QCD forces this distribution to vanish. This is true to all orders in perturbation theory but it fails in the QCD vacuum [$\langle \bar{q}_L q_R \rangle \neq 0$ is the condensate that violates chiral symmetry] and it fails in the nucleon for the same reason. Since the quark chirality flips and since chirality \equiv helicity up to mass terms or further hard interactions, this new distribution will be important when the nucleon helicity flips, *i.e.* in a transverse asymmetry. Thus, there is a new structure function, $h_1(x, Q^2)$, for each flavour of quark and antiquark, which measures the quark momentum distribution in a transversely polarized nucleon weighted by ± 1 depending on whether the quark is polarized parallel or antiparallel to the nucleon. $h_1(x, Q^2)$ cannot be measured in deep inelastic scattering (except as the coefficient of a small quark mass correction) but it appears in the transverse asymmetry for Drell-Yan processes at the dominant “scaling” order.

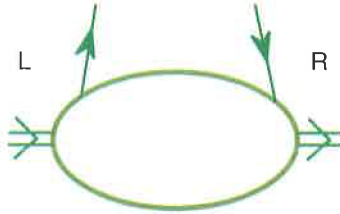


FIGURE 13

Chiral flip distribution which gives $h_1(x, Q^2)$.

The analogy between chiral flip and chiral non-flip processes can be continued at the order of twist-3 corrections. We have considered quark chirality conserving processes in unpolarized (f_1), longitudinally polarized (g_1) and transversely polarized (g_2) targets. So far we have considered quark chirality flip only in a transversely polarized (h_1) target. The other two possibilities yield twist-3 effects — suppressed by $\sim 1/\sqrt{Q^2}$ — because there is a clash between the chirality flip of the quark and the helicity conservation of the nucleon unless quark mass or hard gluon corrections are included. The result are two new twist-3 distributions^(*): $e(x)$ measured in quark chirality flip from a spin averaged target, and $h_2(x)$ measured in the longitudinal target asymmetry involving quark chirality flip. $h_2(x)$ is analogous to $g_2(x)$, as $h_1(x)$ is to $g_1(x)$.

There are two more questions to be addressed: what exactly does $h_1(x)$ measure? And how? The first question has taken some time to formulate and much of the answer is still missing. The second is well on its way to an answer and provides considerable motivation for a versatile spin physics program at a hadronic collider.

When we prepare a nucleon with “transverse spin” we actually mean it is in an eigenstate of the Pauli–Lubansky vector S_μ with \vec{S} transverse to the momentum \vec{P} . It is *not* in an eigenstate of the angular momentum \vec{J} because J_x does not commute with P_z . The quarks in such a nucleon can be classified in the same fashion as eigenstates of the Pauli–Lubansky vector either parallel or antiparallel to the nucleon’s direction. $h_1(x)$ measures the longitudinal momentum distribution of quarks weighted by more or less according to this “transversity” quantum number. The quantity measured by $h_1(x)$ deserves its own name (*transversity*) and must not be confused with transverse spin. Spin is measured by the operator $\bar{q}\gamma_\mu\gamma_5q = \bar{q}_L\gamma_\mu\gamma_5q_L + \bar{q}_R\gamma_\mu\gamma_5q_R$ which preserves quark chirality and has nothing to do with $h_1(x)$ which flips it. The longitudinal and transverse spin distributions in the nucleon are measured by $g_1(x)$ and $g_T(x) \equiv g_1(x) + g_2(x)$, respectively. The difference between the two is the subtle, interaction-dependent distribution $g_2(x)$.

In models $h_1(x)$ is large. In the non-relativistic quark model $h_1(x) = g_1(x)$ but relativistic effects give rise to large differences between the two in models like the MIT bag. Furthermore, quarks and antiquarks contribute rather differently to $h_1(x)$ and $g_1(x)$. The area under $h_1(x)$ measures the nucleon matrix element of a rather simple operator, the “tensor charge” δq

$$\int_0^1 dx (h_1(x) - \bar{h}_1(x)) = \delta q$$

with

$$\left\langle PS \left| \bar{q} \sigma^{\mu\nu} i \gamma_5 q \right| PS \right\rangle = (P^\mu S^\nu - P^\nu S^\mu) \frac{\delta q}{M}, \quad (12)$$

for each quark flavour ($h_1(x)$ and $\bar{h}_1(x)$ refer to quark and antiquark transversity, respectively). Nothing is known about the quark tensor charges $\{\delta q\}$ beyond some simple model calculations.

$h_1(x)$ and $h_2(x)$ are directly measurable in Drell–Yan production of lepton pairs. $h_1(x)$ dominates the transverse–transverse asymmetry (target and beam transversely polarized) [31]

$$A_{TT} = \frac{\sin \theta \cos 2\phi}{1 + \cos^2 \theta} \frac{\sum_a e_a^2 h_1^a(x) \bar{h}_1^a(y)}{\sum_a e_a^2 f_1^a(x) f_1^a(y)}. \quad (13)$$

Here x and y are the longitudinal momentum fractions of the annihilating quarks; θ is the polar angle of the lepton pair in the virtual photon rest frame defined relative to the parton momenta and ϕ is the lepton pair azimuthal angle measured with respect to the transverse spin. The sum on “ a ” covers all quark and antiquark flavours. $h_2(x)$, on the other hand, contributes to the longitudinal–transverse asymmetry [36]

$$A_{LT} = \frac{2 \sin 2\theta \cos \phi}{1 + \cos^2 \theta} \frac{M}{Q} \frac{\sum_a e_a^2 [g_1^a(x) y g_T^a(y) - x h_L^a(x) \bar{h}_1^a(y)]}{\sum_a e_a^2 f_1^a(x) f_1^a(y)}, \quad (14)$$

as does $g_T(y)$. Here $h_L(x) \equiv 1/2 (h_1(x) + h_2(x))$.

Let us finally add some comments on transverse spin. First, note that $h_1(x)$ is a purely quark effect; there is no $h_1(x)$ for gluons. This follows from angular momentum conservation [33]. Hence gluons do not participate in the hard scattering for transverse spin asymmetries, at twist-2. Second, jet production might also be used to probe the quark transversity distributions. However, the partonic level asymmetries \hat{a}_{TT} for the $2 \rightarrow 2$ [39] and $2 \rightarrow 3$ [40] subprocesses are all smaller ($\leq 1/10$) than the corresponding longitudinal asymmetries \hat{a}_{LL} , for quark–quark induced subprocesses. The asymmetry for quark–antiquark induced jet production is higher, but in pp collisions this would not be a valence induced process.

Since the single transverse spin asymmetry, in high x_T single particle production is known to be large, and in QCD this

(*) For other twist-3 contributions related to single transverse spin asymmetries in hadronic collisions see ref. [38].

asymmetry is twist-3, there are likely to be substantial higher twist effects.

4. Conclusions and prospects

The RSC Collaboration has focused detector design studies on the experimental challenge of systematically measuring the longitudinal and transverse spin distributions in the proton. There is considerable work to be done in defining the spin detector (or detectors), and to verify sensitivities to the various parton spin densities with simulation programs. It is clear that the probes to be emphasized are jets, direct photons, W bosons and Drell-Yan pairs. The measurements will consist of transverse and longitudinal single and double spin asymmetries.

It is possible that the RHIC detectors, which have been proposed for heavy ion physics, would be acceptable for high-luminosity polarized proton studies. The high-track multiplicity which will characterize the working environment for heavy-ion detectors will impose design considerations similar to those required for high-luminosity polarized proton experiments. Thus, the RSC Collaboration is considering using (possibly augmenting) RHIC detectors for spin-physics experiments. Alternatively, for direct photon and jet detection, a high-rate detector similar to UA2 Experiment at CERN has been considered.

As an example, the asymmetry of direct photon production is related to $\Delta G(x)$, the longitudinal spin of the proton carried by gluon fields. Direct photon events, either with or without away side-jet detection, provide information about $\Delta G(x)$ or integrals of $\Delta G(x)$.

As a compromise to cost, a coarse-grained electromagnetic calorimeter has been studied for use in this measurement. Large cell sizes, with solid angles in the range of 17^2 to 32^2 mrad² have been studied in detail. The coalescence of gammas from π^0 decays is a greater problem as the cell size is increased. This reduces the signal to background ratio but still allows observation of the direct photon asymmetry. A preconverter, with 1 cm scintillator strips located just before shower maximum somewhat improves the situation for a modest incremental cost.

Hadron jets can be studied either in the conventional way with an EMC plus a hadron calorimeter or with a tracking detector in a magnetic field plus an electromagnetic detector. The loss of neutral hadrons in the later case appears not to compromise the physics of interest. Due to the finite size of jets, the jet detector must be larger than the fiducial acceptance in rapidity or in ϕ for detectors that do not cover 2π . Also, there is an interest in events which are asymmetric in x_1 and x_2 , for example a large x up-quark interacting with a low x gluon. These would also increase the rapidity coverage to beyond a minimal ± 1 , probably to ± 2 .

The Drell-Yan interactions provide information on the sea quark and transversity spin distributions. Statistics may limit these measurements to dilepton masses just above the J/ψ . New ideas, involving exotic techniques for observing the transverse

spin structure in high statistics single-spin asymmetry measurements with additional observation of final state-jet substructure are under study. If such measurements are found to be possible, new requirements on jet detectors may emerge. The integration and optimization of features required for the specific aspects of Drell-Yan, direct photon and jet detection in a new or existing detector presents an exciting challenge to the members of the RSC Collaboration.

Acknowledgements

This work was supported in part by the Department of Energy under Contract Numbers W-31-109-ENG-38 (D. Underwood and A. Yokosawa), DE-AC02-76CH00016 (G. Bunce, Y. Makdisi and M. Tannenbaum), DE-AC02-76ER03069 (R. Jaffe) and DE-FG02-90ER-40577 (J. Collins), by the National Science Foundation under Grant Numbers PHY-8815259 (S. Heppelmann), and PHY-9001744 (R. Robinett), and by the Texas National Research Laboratory Commission (J. Collins and R. Robinett).

References

- [1] Y.S. Derbenev and A.M. Kondratenko, *Sov. Phys. Doklady*, 20 (1976) 562;
Y.S. Derbenev et al., *Particle Accelerators* 8 (1978) 115.
- [2] A.D. Krisch, *Phys. Rev. Lett.* 63 (1989) 1137 (for the first experimental tests of the Siberian snake concept).
- [3] S.Y. Lee and E.D. Courant, *Phys. Rev. D* 41 (1990) 292 (and references therein);
S.Y. Lee and E.D. Courant, Brookhaven preprint AD/RHIC-63.
- [4] Proceedings of the Polarized Collider Workshop, Penn State University (1990) eds J. Collins, S. Heppelmann and R.W. Robinett, AIP conf. proc. No. 223, American Institute of Physics, New York (1991).
- [5] G. Bunce, in ref. [4] 147.
- [6] V. Hughes, in ref. [4] 51;
A.V. Efremov, in ref. [4] 80;
A. Manohar, in ref. [4] 90.
- [7] RHIC Spin Collaboration, Letter of Intent (April 1991)^(*).

(*) As of this writing, RSC consists of the following physicists from 15 institutions: *Argonne* (M. Beddo, D. Hill, D. Grosnick, D. Lopiano, H. Spinka, D. Underwood and A. Yokosawa); *Brookhaven* (G. Bunce, A. Carroll, E. Courant, R. Fernow, Y.Y. Lee, D. Lowenstein, Y. Makdisi, L. Ratner, T. Roser, M. Sakitt, A. Sambamurti and M. Tannenbaum); *Dubna* (A.V. Efremov); *Indiana* (S.Y. Lee); *Genova* (M. Conte); *Helsinki* (N. Törnqvist); *KEK* (S. Hiramatsu, Y. Mori and H. Sato); *Kyoto* (H. Enyo, K. Imai and A. Masaïke); *Marseille* (J. Soffer); *MIT* (R. Jaffe); *Padova* (M. Pusterla); *Penn State* (J. Collins, S. Heppelmann, G. Ladinsky, E. Minor and R. Robinett); *Serpukhov* (Y. Arestov, B.V. Chuiko, A.M. Davidenko, A.A. Derevschikov, O.A. Grachov, A.K. Likhoded, A.P. Meschanin, S.B. Nurushhev, V.L. Rykov, A.G. Ufimtzev and A.N. Vasiliev); *Trieste* (A. Penzo and P. Schiavon); *UCLA* (G. Igo) and *unaffiliated* (D. Sivers).

■ References (cont'd)

- [8] C. Bourrely, J.Ph. Guillet and J. Soffer, Spin effects with polarized protons at RHIC, Nucl. Phys. B361 (1991) 72.
- [9] J. Collins, proc. of the Conference on the Intersections of Nuclear and Particle Physics, Tuscon, Arizona, American Inst. of Ph. (1991) to appear;
R.W. Robinett, proc. of PF91, Vancouver, Canada, ed. World Scientific (1991) to appear.
- [10] J.G. Alessi et al., AIP conf. proc. 187 (1988) 1221.
- [11] E880, The effect of a partial snake on polarization at the AGS (1991).
- [12] S.Y. Lee, Nucl. Inst. and Meth. A306 (1991) 1.
- [13] S.Y. Lee and S. Tepikian, Phys. Rev. Lett. 56 (1986) 1635.
- [14] H. Primakoff, Phys. Rev. 81 (1951) 899;
A. Halprin, C.M. Anderson and H. Primakoff, Phys. Rev. 152 (1966) 1295;
L. Stodolsky, Phys. Rev. 144 (1966) 1145;
G. Faldt, Nucl. Phys. B41 (1972) 591.
- [15] B. Margolis and G.H. Thomas, High-energy polarized proton beams, AIP conf. proc. 42 (1978) 173.
- [16] D.G. Underwood, ANL-HEP-PR-77-56 (1977).
- [17] D.C. Carey et al., Phys. Rev. Lett. 64 (1990) 357.
- [18] J. Schwinger, Phys. Rev. 73 (1948) 407.
- [19] C. Bourrely and J. Soffer, Lett. al Nuovo Cimento 19 (1977) 569.
- [20] N. Akchurin et al., Phys. Lett. B229 (1989) 299, and references therein.
- [21] B.Z. Kopeliovich and L.I. Lapidus, Yad. Fiz. 19 (1974) 218 (Sov. J. Nucl. Phys. 19 (1974) 114).
- [22] N.H. Buttimore, E. Gotsman and E. Leader, Phys. Rev. D18 (1978) 694.
- [23] N.H. Buttimore, proc. of the 6th Int. Symp. on High-Energy Spin Physics, Marseille, ed. J. Soffer, Journal de Physique, C2 46 (1985) 643.
- [24] N. Akchurin et al., to be published.
- [25] D.L. Adams et al., Phys. Lett. B264 (1991) 462.
- [26] C. Bourrely et al., Phys. Rep. 177 (1989) 319, and errata to preprint CPT-87/P.2056 (December 1990).
- [27] J. Ashman et al., EMC, Nucl. Phys. B328 (1989) 1.
- [28] E. Berger and J. Qiu, Phys. Rev. D40 (1989) 778.
- [29] M.A. Doncheski, R.W. Robinett and L. Weinkauff, Phys. Rev. D44 (1991) 2717.
- [30] X. Ji, proc. of PF91, Vancouver, Canada, ed. World Scientific (1991) to appear.
- [31] J. Ralston and D.E. Soper, Nucl. Phys. B152 (1979) 109.
- [32] J. Kodaira et al., Nucl. Phys. B159 (1979) 99;
A.P. Bukhvostov, E.A. Kuraev and L.N. Lipatov, Sov. Phys. JETP 60 (1984) 22.
- [33] X. Artru and M. Mekhfi, Zeitschr. für Phys. C45 (1990) 669.
- [34] J. Collins, Penn State preprint (1990) and private communication.
- [35] J.L. Cortes, B. Pire and J.P. Ralston, Polarized Collider Workshop, in ref. [4] 184.
- [36] R.L. Jaffe and X. Ji, Phys. Rev. Lett. 67 (1991) 552.
- [37] R.L. Jaffe and X. Ji, Phys. Rev. D43 (1991) 724;
R.L. Jaffe, Comm. in Nucl. Part. Phys. 19 (1990) 239 and references therein.
- [38] A.V. Efremov and O.V. Teryaev, Phys. Lett. B150 (1985) 383 and references therein;
J. Qiu and G. Sterman, Phys. Rev. Lett. 67 (1991) 2264.
- [39] K. Hidaka, E. Monsay and D. Sivers, Phys. Rev. D19 (1979) 1503.
- [40] R.W. Robinett, Pen State preprint PSU/TH/96 (1991).

■ Addresses:

D. Underwood and A. Yokosawa
Argonne National Laboratory
Argonne, IL 60439 (USA)

G. Bunce, Y. Makdisi and M. Tannenbaum
Brookhaven National Laboratory
Upton, NY 11973 (USA)

S.Y. Lee
Department of Physics
Indiana University
Bloomington, IN 47405 (USA)

J. Soffer
Centre de Physique Théorique
CNRS, Luminy Case 907
F-13288 Marseille Cedex 9 (France)

R. Jaffe
Department of Physics
Massachusetts Institute of Technology
Cambridge, MA 02139 (USA)

J. Collins, S. Heppelmann and R.W. Robinett
Department of Physics
Penn State University
University Park, PA 16802 (USA)

■ Received on December 1991.